Electrical Characterization of 65 W Cubic Sonoreactor with Horizontally Stacked Transducers

Pansak KERDTHONGMEE[(1)], Chat PHOLNAK[(1), (2)]

Chitnarong SIRISATHITKUL[(1)], Sorasak DANWORAPHONG[(1)]

[(1)] *Department of Physics, School of Science*
Walailak University
Nakhon Si Thammarat, Thailand; e-mail: chitnarong.siri@gmail.com

[(2)] *Department of Physics, Faculty of Science*
Thaksin University
Phatthalung, Thailand

A sonoreactor was assembled with stacked lead zirconate titanate transducers. These transducers were attached on one side of a $10 \times 10 \times 10$ cm^3 chamber and driven by an integrated circuit power amplifier. The impedance of the reactor was analyzed in order to determine a matching inductance. The electrical frequency could be varied from 20 to 50 kHz and the electrical output power was adjustable up to 65 W. The highest power was obtained in the case of resonance at 31 kHz and the maximum temperature at the heat sink of the amplifier rose to 42.0°C. Both acoustic cavitation and mechanical effects could be utilized in this sonoreactor for a variety of purposes including sonochemical synthesis, ultrasonic cleaning and microbial cell disruption.

Keywords: sonoreactor; dual stack transducer; low frequency ultrasound; RLC circuit; resonant frequency.

1. Introduction

Ultrasound has widely been implemented with either high frequency or high power. The ultrasonic characterization for non-destructive testing and imaging usually employs a low power signal with frequency up to 70 MHz. By contrast, the power of order of 10 W is generally required in ultrasonic cleaning (SAIKIA *et al.*, 2014) dyeing (GUESMI *et al.*, 2013), food processing (KENTISH, FENG, 2014), natural product extraction (ESCLAPEZ *et al.*, 2011), microbial cell disruption (BORTHWICK *et al.*, 2005), acoustic cavitation (KHMELEV *et al.*, 2015) and sonochemistry (SON *et al.*, 2012). Moreover, applications of power exceeding 100 W are common in biodegradation (ZAWIEJA, WOLNY, 2011) and alloy treatment (SHAO *et al.*, 2012). During the sonication, molecules and materials in liquid media receive power transfer from both mechanical vibration and acoustic cavitation mechanisms. With only moderate temperature rise in the media, these mechanical and sonochemical effects benefit several processes.

In the case of high acoustic power demand, the design of a sonoreactor has to be optimized for maximum ultrasonic power and minimum loss. Geometrical factors including the size and shape of reactors were experimentally investigated (NIKITENKO *et al.*, 2007; KIM *et al.*, 2014; LORANGER *et al.*, 2011; JORDENS *et al.*, 2013; THANGAVADIYEL *et al.*, 2013; MEMOLI *et al.*, 2012) and simulated (JORDENS *et al.*, 2013; NIAZI *et al.*, 2014). There is also a large variation in designs, e.g. the bath/flow through type, immersed probe/external sonication, single/multiple transducers. Effects of operational factors such as the liquid height were also studied (DE LA ROCHEBROCHARD *et al.*, 2012; SON *et al.*, 2009).

The acoustic power transferred in sonoreactors can be measured by means of calorimetry, pressure or electrical measurements (NIKITENKO *et al.*, 2007; PETOSIC *et al.*, 20011; SAEZ *et al.*, 2005; HALLEZ *et al.*, 2007). Since the power dissipated in the sonoreactor is dependent on the electrical power supplied to the ultrasonic transducer, attentions should be paid to the

transducer circuit. To drive these transducers, the impedance tuning circuit is often employed to amplify the low power signal from the function generator. In this work, a sonoreactor with adjustable frequency and power has been assembled and its electrical characteristics including the incurred heat were studied. The main propose of this sonoreactor is to sonochemically synthesize ZnO (Pholnak *et al.*, 2014) but its application can be extended with the knowledge of its characteristics.

2. Experimental

2.1. Sonoreactor

Figure 1 illustrates the installation of dual stack transducers at one side of a cubic chamber. The $10 \times 10 \times 10$ cm^3 chamber was made by folding a 1 mm thick stainless steel sheet. The transducers were 2 lead zirconate titanate (PZT, Chanel Industries, USA) disks of 7 cm in diameter and 1 cm in thickness. They were placed into the annular acrylics and covered by 2 electrodes, one of which was grounded and the other was the source electrode.
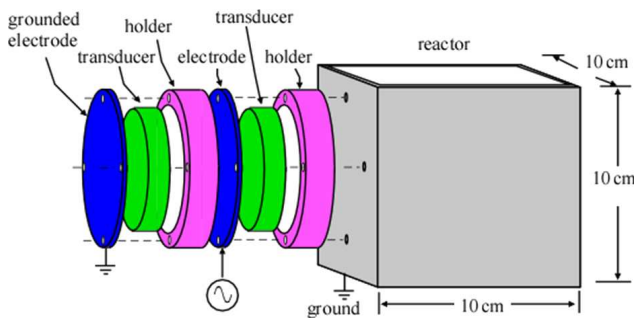

Fig. 1. Schematic diagram of dual stack transducer assembly attached to the cubic chamber.

With this horizontally irradiated configuration, more transducers can further be added at other sides and an external heat source may be supplied at the base. By stacking the transducers, the moderate power can be used efficiently (Kim *et al.*, 2014). Furthermore, the compact size of this system selected to match the dimensions of PZT transducers and standard heat source reduces the power loss (Jordens *et al.*, 2013).

The electrical impedance of this sonoreactor was investigated by using an impedance analyzer (Hewlett Packard, HP4912A). In Fig. 2, the measured electrical impedance exhibits a large variation in response to the change in frequency between 20 and 50 kHz. The peak impedance of 2.25 kΩ is observed at 42 kHz. By either increasing or decreasing this frequency, the impedance rapidly drops. The impedance becomes the minimum and is close to zero when the frequency is around 30.5 kHz. The phase angle is plotted as a function of
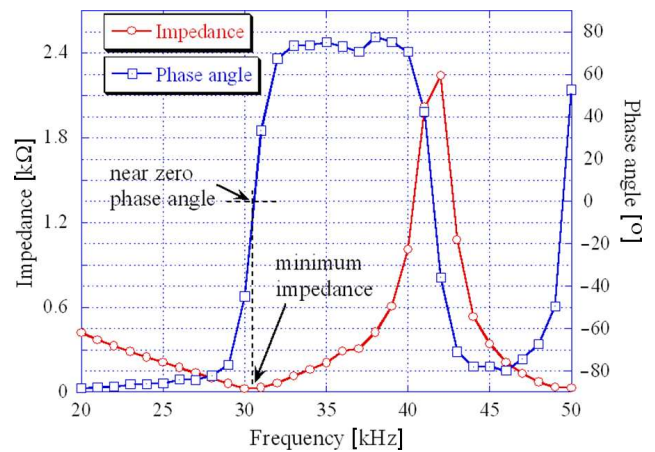

Fig. 2. Electrical impedance and the phase angle measured as a function of the driven frequency.

the frequency on the same scale in Fig. 2 to explain the variation of impedance. The minimum impedance occurs when the phase angle is nearly zero.

2.2. Power amplification topology

An inductor was connected to the stack transducers so that the electrical loss during the operation of the sonoreactor could be minimized at the resonance condition of the RLC circuit. The value of matching inductance can be calculated at the resonant frequency (f_r) as follows;

$$f_r = \frac{1}{2\pi\sqrt{LC}},$$

where L is the inductance and C is the capacitance of the sonoreactor. The latter was determined from the impedance at 30.5 kHz in Fig. 2 as 18.8 nF. It follows that the L was 1.5 mH. The matching inductor was then made by winding 200 turns of laminated copper wires on a 10 cm-diameter PVC air core.

In order to adjust both frequency and power for different demands, the power amplification topology shown in Fig. 3 was selected rather than the switching mode power source. The integrated circuit (IC) (Sanyo Electric, STK4048II) was used as the amplifier. The advantages of this wide-bandwidth power amplifier IC are its simplicity, low price and relatively low internal power loss. An enhanced output signal was supplied to
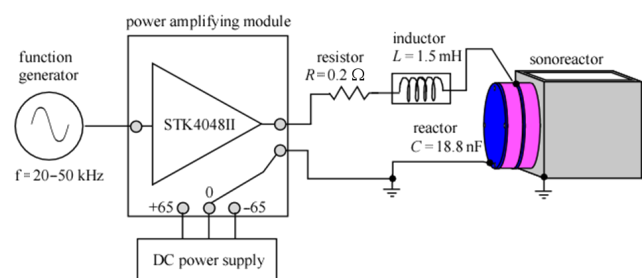

Fig. 3. Power amplification topology for sonoreactor.

the *RLC* equivalent circuit incorporating the 18.8-nF stacked transducers, the 0.2-Ω resistor and the 1.5-mH inductor.

2.3. System setting

The system in Fig. 4 comprises the sonoreactor with dual stack transducers, a matching inductor, a power amplifying module and a function generator (Agilent 33220A). The frequency of signal for this circuit was regulated from 20 to 50 kHz by the function generator. A digital multimeter (Agilent 34401A) was used as an ammeter to measure the input current. The waveform and voltage drop across the transducer as well as the RLC circuit were monitored by the oscilloscope (GW Instek GDS-2204) and the electrical current was measured by a digital multimeter. The power output was then calculated from the product of measured current and voltage drop. During the operation, the temperature of the power amplifying module was also measured.
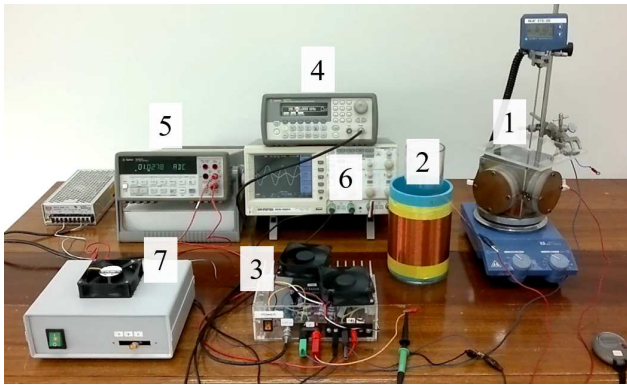
Fig. 4. Photograph showing the system setup; (1) reactor, (2) 1.5 mH inductor, (3) power amplifier, (4) function generator, (5) ammeter, (6) oscilloscope and (7) DC power supply.

3. Results and discussion

The resonant frequency around 30 kHz is confirmed by measuring the voltage drop across the transducer as a function of the frequency. When a constant 10 mV input is used, the peak voltage of 3500 mV is obtained at 31 kHz and the curve in Fig. 5 shares similar characteristics with that in Fig. 2. The determination of resonant frequency has to be very precise and thus, the frequency in Fig. 5 was finely scanned to detect the peak position. The resonant frequency was also confirmed by independent impedance and phase measurements in Fig. 2. The peak in Fig. 5 occurs at the frequency comparable (less than ±1 KHz) to the condition with phase and impedance close to zero. To a lesser extent, the uncertainty in resonant frequency also arises from the uncertainty in L and C quantities.
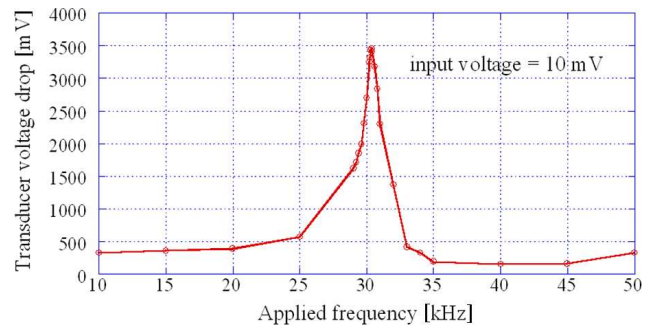
Fig. 5. Voltage drop across the dual stack transducer measured as a function of the driven frequency.

To utilize the maximize power available in this system, the characteristics of the sonoreactor at the resonant frequency is further investigated. By varying the input voltage between 200 and 3000 mV (with the deviation of ±40 μV), the electrical power output is increased from 4 up to 65 W with the total harmonic distortion (THD) of less than 0.5%. The plot of power output against input voltage in Fig. 6 exhibit 3 trends meaning that the linear variation is observed in 3 regimes. Beyond the first regime (I) of less than 10 W, the power output is sharply increased in the middle regime (II) whose slope is the highest and equivalent to 40 W/V. Since the cavitation is initiated above 20 W with observable bubbles, this low frequency ultrasonic device will be useful for sonochemical synthesis and ultrasonic cleaning. However, its size may limit its use for commercial ultrasonic dyeing and food processing
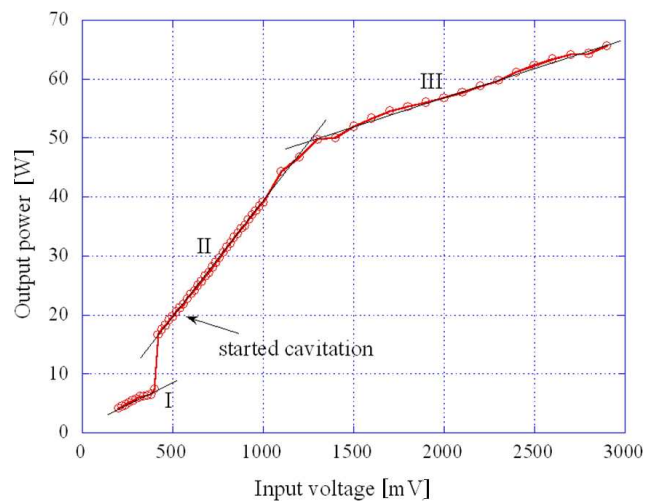
Fig. 6. Variation of electrical output power of sonicator with the input voltage.

Figure 7 demonstrates the change in heat sink temperature of the IC as the operation is progressed. To obtain the testing power of 60 W, the circuit was gradually adjusted in a period over 10 s. By that time, the temperature had reached 30.0°C which was marked as a starting temperature with the measurement de-
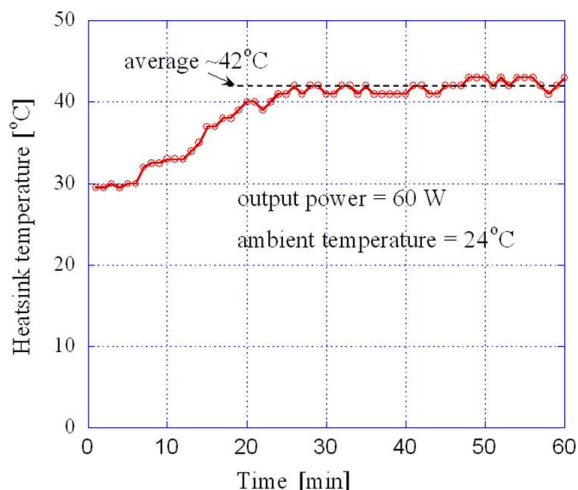
Fig. 7. Variation of heat sink temperature of the amplifier with the operation time.

viation of $\pm 0.1°C$. In the first 25 min, the temperature steadily rises from 30.0 to over 40.0°C. The temperature then fluctuates around 42.0°C for the next 35 min of testing. Such level does not pose the overheating problem in the system and a stable sonication is achieved.

4. Conclusions

A cost effective low frequency sonication system was developed with the 18.8-nF dual stack transducers treated as a part of the *RLC* circuit. The signal was then enhanced by the power amplifying module. The resonant frequency of the sonoreactor was at 30.5 kHz. At the resonance, the electrical power from the amplifier can be supplied to the reactor with the maximum of 65 W and high stability. This compact system is capable of working with different variations of ultrasonic transducer between 20 and 50 kHz.

Acknowledgments

References

1. Borthwick K.A.J., Coakley W.T., McDonnell M.B., Nowotny H., Benes E., Gröschl M. (2005), *Development of a novel compact sonicator for cell disruption*, Journal of Microbiological Methods, **60**, 2, 207–216.

2. de La Rochebrochard S., Suptil J., Blais J.F., Naffrechoux E. (2012), *Sonochemical efficiency dependence on liquid height and frequency in an improved sonochemical reactor*, Ultrasonics Sonochemistry, **19**, 2, 280–285.

3. Esclapez M.D., Garcia-Perez J.V., Mulet A., Carcel J.A. (2011), *Ultrasound-assisted extraction of natural products*, Food Engineering Reviews, **3**, 2, 108–120.

4. Guesmi A., Ben Hamadi N., Ladhari N., Sakli F. (2013), *Sonicator dyeing of modified acrylic fabrics with indicaxanthin natural dye*, Industrial Crops and Products, **42**, 1, 63–69.

5. Hallez L., Touyeras F., Hihn J.Y., Klima J. (2007), *Energetic balance in an ultrasonic reactor using focused or flat high frequency transducers*, Ultrasonics Sonochemistry, **14**, 6, 739–749.

6. Jordens J., Honings A., Degreve J., Braeken L., Van Gerven T. (2013), *Investigation of design parameters in ultrasound reactors with confined channels*, Ultrasonics Sonochemistry, **20**, 6, 1345–1352.

7. Kentish S., Feng H. (2014), *Applications of power ultrasound in food processing*, Annual Review of Food Science and Technology, **5**, 263–284.

8. Khmelev S.S., Khmelev V.N., Golykh R.N., Shalunov A.V. (2015), *Development and research of concentrator-sonotrode with increased radiating surface*, Archives of Acoustics, **40**, 1, 129–135.

9. Kim E., Cui M., Jang M., Park B., Son Y., Khim J. (2014), *Investigation of sonochemical activities at a frequency of 334 kHz: the effect of geometric parameters of sonoreactor*, Ultrasonics Sonochemistry, **21**, 4, 1504–1511.

10. Loranger E., Paquin M., Daneault C., Chabot B. (2011), *Comparative study of sonochemical effects in an ultrasonic bath and in a large-scale flow-through sonoreactor*, Chemical Engineering Journal, **178**, 359–365.

11. Memoli G., Gelat P.N., Hodnett M., Zeqiri B. (2012), *Characterisation and improvement of a reference cylindrical sonoreactor*, Ultrasonics Sonochemistry, **19**, 4, 939–952.

12. Niazi S., Hashemabadi S.H., Noroozi S. (2014), *Numerical simulation of operational parameters and sonoreactor configurations for the highest possibility of acoustic cavitation in crude oil*, Chemical Engineering Communications, **210**, 1340–1359.

13. Nikitenko S.I., Le Naour C., Moisy P. (2007), *Comparative study of sonochemical reactors with different geometry using thermal and chemical probes*, Ultrasonics Sonochemistry, **14**, 3, 330–336.

14. Petosic A., Svilar D., Ivancevic B. (2011), *Comparison of measured acoustic power results gained by using three different methods on an ultrasonic low-frequency device*, Ultrasonics Sonochemistry, **18**, 2, 567–576.

15. Pholnak C., Suwanboon S., Sirisathitkul C. (2014), *Evolution and temperature dependence of ZnO formation by high power sonication*, Journal of Materials Science: Materials in Electronics, **24**, 5014–5022.

16. Saez V., Frías-Ferrer A., Iniesta J., Gonzalez-Garcia J., Aldaz A., Riera E. (2005), *Chacterization of a 20 kHz sonicator. Part I: Analysis of mechan-*

ical effects by classical and numerical methods, Ultrasonics Sonochemistry, **12**, 1–2, 59–65.

17. SAIKIA B.K., DUTTA A.M., SAIKIA L., AHMED S., BARUAH B.P. (2014), *Ultrasonic assisted cleaning of high sulphur Indian coals in water and mixed alkali*, Fuel Processing Technology, **123**, 107–113.

18. SHAO Z., LE Q., ZHANG Z., CUI J. (2012), *Effect of ultrasonic power on grain refinement and purification processing of AZ80 alloy by ultrasonic treatment*, Metals and Materials International, **18**, 209–215.

19. SON Y., LIM M., SONG J.H., KHIM J. (2009), *Liquid height effect on sonochemical reactions in a 35 kHz sonoreactor*, Japanese Journal of Applied Physics, **48**, 07GM16.

20. SON Y., LIM M., KHIM J., ASHOKKUMAR M. (2012), *Acoustic emission spectra and sonochemical activity in a 36 kHz sonoreactor*, Ultrasonics Sonochemistry, **19**, 1, 16–21.

21. THANGAVADIYEL K., OWENS G., LESNIEWSKI P.J., OKITSU K. (2013), *Influence of reactor shapes on residence time distribution and methyl orange degradation efficiency in a continuous process under indirect 200 kHz sonication*, Industrial & Engineering Chemistry Research, **52**, 18175–18183.

22. ZAWIEJA I., WOLNY L. (2011), *Effect of sonicator power on the biodegradability of sewage sludge*, Rocznik Ochrona Środowiska, **13**, 1719–1730.